ICSV14
Cairns • Australia
9-12 July, 2007

BEAMFORMING IN HIGHLY REVERBERANT WIND TUNNELS POSSIBILITIES AND LIMITATIONS

Benjamin Fenech, Kenji Takeda

School of Engineering Sciences
University of Southampton
SO17 1BJ, UK

ktakeda@soton.ac.uk

Abstract

Closed-section hard-walled wind tunnels are routinely used for aerodynamic testing during the early stages of vehicle design. The use of microphone arrays and beamforming processing in such environments can yield useful source localisation information; yet there are concerns as to the consistency of quantitative results from such methods when compared to anechoic open-jet tunnel testing. Higher background noise levels, microphones in contact with the turbulent boundary layer, and the highly reverberant nature of the measuring environment are of particular concern. In this paper we show that accurate results in closed-section wind tunnels are still possible using the cross-spectral matrix diagonal removal (DR) technique, and with de-reverberation. With DR, improvements in beamformer's accuracy up to 10 dB can be achieved when compared to standard beamforming. De-reverberation gives an additional 10 dB improvement, and provided that the noise contamination to the microphone pressure data is somewhat suppressed, errors within $\pm$1dB can be expected. Both of these methods do not require any additional changes to the physical infrastructure of the measuring environment.

1. INTRODUCTION

In the last decade, significant progress in aeroacoustic measurements has been made using phased microphone arrays, especially in the post-processing techniques based on frequency-domain beamforming [1, 2, 3]. Most measurements tend to be carried out in large, open-jet facilities, where microphones are situated out of flow, and the test section boundaries are acoustically treated to reduce background noise levels and reflections. However, measurements in closed-section wind tunnels can still yield useful results [3, 4]. Such measurements offer the possibility of back-to-back testing with the routine aerodynamic measurements performed at the initial stages of an aircraft development cycle. These wind tunnels also benefit from shorter setup times, and in most cases, shorter distances between array and model[2].

[2]Besides the obvious advantage of a better beamforming resolution, a shorter distance between array and model means less information lost due to coherence loss.

For many, the biggest concern for tests in closed section wind tunnels is the level of correlation between the beamforming levels and the true aeroacoustic source strengths. This is a justified preoccupation, given that for example, microphones are subjected to levels that are up to 50 dB higher [5] than their open-jet equivalents[3]. The most popular technique to overcome this effect consists of altering the diagonal of the cross spectral matrix (CSM) of the measured pressures. Whilst this technique is proven to be effective at reducing the boundary layer noise, to the authors' best knowledge there is no formal documented study of how it effects the beamformer results.

Further errors can be expected from the contribution of reflections which build up in a closed-tunnel's hard-walled test section. The beamformer can be modified to model these reflections and "de-reverberate" the space. In this paper an image source model is used to model the reflection from an enclosed space, and a number of simulations are presented to show any potential benefits which can be achieved using this method, together with its sensitivity to errors.

2. DE-REVERBERATION

2.1. Background

Conventional frequency-domain beamforming, as applied to random noise with stationary statistical properties, can be expressed as [6]

$$Y_{\text{opt}} = \left[\mathbf{g}^{\dagger}\mathbf{g}\right]^{-2} \mathbf{g}^{\dagger}\mathbf{S_{pp}}\mathbf{g}, \tag{1}$$

where Y_{opt} is the beamformer output at a point in space $\vec{y}_p$, $\mathbf{S_{pp}}$ is the cross spectral matrix (CSM) of measured pressures, $\mathbf{g}$ is the vector of Green's functions relating $\vec{y}_p$ to each microphone and $[\cdot]^{\dagger}$ denotes a complex conjugate transpose. The diagonal of $\mathbf{S_{pp}}$ is frequently replaced by zeros or by an off-diagonal column average to reduce the contribution of incoherent noise from the measurements [7, 8].

For simplicity Green's functions are often assumed to be free-space Green's functions for a monopole, which are easy to compute. Holland and Nelson [6] have shown that this gives rise to errors when measuring in a semi-reverberant space. Using measured Green's functions they successfully "de-reverberated" the space and nullified the error. It is reasonable to assume that in a highly reverberant space such as a closed-section wind tunnel errors will be more significant, and de-reverberation should be used in these cases as well. Preliminary tests have shown that errors are indeed significant, and that de-reverberation can help to reduce errors, as shown in Fig. 1.

Unfortunately, measuring Green's functions for a large number of microphone-grid point locations requires a lot of time and effort. A possible alternative is to model the wind tunnel test section, and use predicted Green's functions rather than measured ones.

2.2. The Image Source Model (ISM)

There are various ways how to model the sound field within the bounded space representing the wind tunnel test section. Since beamforming is most effective at high frequencies, an image

[3]The drastic reduction in levels in state-of-the-art aeroacoustic wind tunnels is due to a number of factors, amongst which a quieter background noise source (wind tunnel fan), sound attenuation along the wind tunnel path, and microphones which are out of flow.

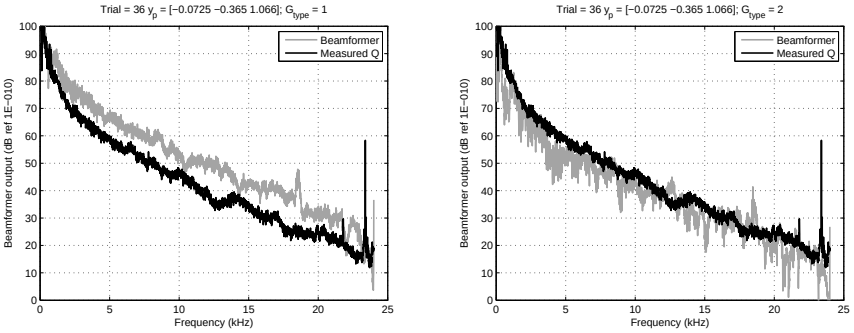

(a) Standard Beamforming (b) Beamforming with de-reverberation

Figure 1. Comparison between the measured source strength of a source and the beamformer's output when focused on the source, with and without de-reverberation. Measurements in a closed-section hard-walled wind tunnel, without flow. Further details in Ref. [9].

source model is probably the most appropriate. Integrating such a model in the microphone array measurement system is easy to accomplish, since it requires zero extra time during wind tunnel testing; furthermore the additional computational time is negligible. The disadvantages are that wind tunnel test sections might have complex cross-sections which are difficult to model, and surface discontinuities might give rise to errors. Furthermore it is practically impossible to model the scattering and diffraction effects induced by the vehicle component under test.

The simplest case to model is a rectangular duct bound by rigid planar walls of infinite extent. A point source in this duct gives rise to a twofold infinity of image sources, all lying in a plane transverse to the duct [10]. In practice only a finite number of images have to be taken into account, since the data acquired is of finite duration. Moreover, energy is dissipated with each reflection, which means that higher-order image sources have a smaller contribution on the final signal.

Assuming point sources, the pressure $p(\vec{x}_m)$ at the mth microphone of an M-channel microphone array can be calculated from the contribution of the "true" source of strength q_s at $\vec{y}_0$, plus all the resulting image sources,

$$p(\vec{x}_m) = \frac{\mathrm{i}\omega\rho_0 q_s}{4\pi}\left[\frac{\mathrm{e}^{-\mathrm{i}kr_0}}{r_0} + \frac{\mathrm{e}^{-\mathrm{i}kr_1}}{r_1} + \frac{\mathrm{e}^{-\mathrm{i}kr_2}}{r_2} + \ldots\right], \tag{2}$$

where $r_j = |\vec{y}_j - \vec{x}_m|$ and $\vec{y}_j$ defines the location of the jth image source. The effective Green's function can therefore be expressed as

$$G(\vec{x}_m|\vec{y}_p) = \frac{p(\vec{x}_m)}{q_s} = \frac{\mathrm{i}\omega\rho_0}{4\pi}\sum_{j=0}^{N}\frac{\mathrm{e}^{-\mathrm{i}kr_j}}{r_j} \quad j = 0, 1, 2, \ldots, \tag{3}$$

where $y_p = y_0$ is the grid point location.

In practice there will be some form of energy attenuation, especially for the higher-order image sources at high frequencies. The easiest way how to integrate this in the above model is to assign a real-valued quantity $\alpha(\omega)$ together with an integer n_j representing the number of boundary interactions corresponding to the j^{th} image source. Inserting this in Eq. 3, and taking into account the presence of a mean flow $\vec{U}$ (such that the Green's functions become a solution

to the convected wave equation [11]), gives

$$G(\vec{x}_m|\vec{y}_p) = \frac{\mathrm{i}\omega\rho_0}{4\pi}\left[\frac{\mathrm{e}^{-\mathrm{i}\omega\sigma_{m0}}}{R_{m0}} + \sum_{j=1}^{N}\frac{[1-\alpha]\,n_j\mathrm{e}^{-\mathrm{i}\omega\sigma_{mj}}}{R_{mj}}\right], \tag{4}$$

where

$$R_{mj} = \sqrt{\left[\vec{M}\cdot(\vec{x_m}-\vec{y_j})\right]^2 + \beta^2\|\vec{x_m}-\vec{y_j}\|^2}, \tag{5}$$

$$\vec{M} = \frac{\vec{U}}{c_0} \quad \text{and} \quad \beta = \sqrt{1-\|\vec{M}\|^2}. \tag{6}$$

σ_{mj} represents the time delay corresponding to the convected wave from the j^{th} source to the m^{th} microphone.

2.3. Implementation

A number of beamforming simulations were carried out in Matlab to *(a)* gain more insight into the effectiveness of the CSM DR technique and (b) test the potential benefits of dereverberation, and its sensitivity to errors. The simulations were based on the SotonArray beamforming code [12], which is currently used to perform microphone array testing in the wind tunnels at the University of Southampton. The original code was modified in two ways: first the simulated pressure data is computed directly in the frequency domain using a predefined value of q_s and the user choice of Green's functions. Secondly, the beamforming processing is carried out at one grid point ($\vec{y}_p = \vec{y}_0$) for a frequency vector from 0 to 20 kHz at 5 Hz intervals[4]. An image source model, based on Eq. 4, was integrated in the code to carry out de-reverberation. The model was based on a rectangular duct with a cross-section of 2.1×1.5 m. Image sources were grouped in order numbers, which refer to the number of expanding rectangles encompassing the image sources[5]. The dissipative constant α was set to the following values: 0.01 for $f \leq 1$ kHz, 0.1 for $1\,\text{kHz} < f \leq 2\,\text{kHz}$, 0.15 for $2\,\text{kHz} < f \leq 4\,\text{kHz}$, 0.2 for $4\,\text{kHz} < f \leq 8\,\text{kHz}$ and 0.4 for $f > 8$ kHz.

Errors of different magnitude were introduced in some parameters, including source and receiver coordinates, wind tunnel cross-section, Mach number and the simulated pressure data. Errors in source position and test section consisted of a fixed "bias" value, whereas errors in Mach number were expressed as a percentage of the original value. Microphone coordinates errors were randomly generated to a predefined maximum amount. Errors in the simulated pressure data p_{sim} were computed by $p_{\text{err}} = re_{\text{max}}p_{\text{sim}}$, where $-1 \leq r \leq 1$ is a randomness factor, and e_{max} is a fraction representing the maximum error. Random numbers were generated using Matlab's default random number generator, which uses a modified version of Marsaglia's subtract with borrow algorithm. The random number generator was reset to the same initial state for each test case, to ensure that the same errors were used.

Various arrays were used in the simulations, all assumed to be mounted vertically on the shorter dimension, with the centre of the array at 0.65 m from the ground. The reference array aperture size is 0.7 m, and sensors are distributed using an aperiodic design based on the multi-

[4]Normally beamforming is carried out at a single frequency for a large number of grid points.

[5]Further details can be found in Fenech and Takeda [9].

arm log spiral [8]. Further simulations were done using 1.25 m-diameter aperiodic arrays and arrays with a regular sensor distribution. The reference source position was randomly chosen as [-0.07,-0.365,1.066], with the origin at the array centre.

2.4. Known Limitations

One of the main assumption when generating the image sources is that of infinite planar walls; this assumption breaks down at the lower frequencies. With the chosen geometry, the shortest dimension (1.5 m) is equivalent to ten wavelengths at approx. 2.3 kHz, and it should be reasonable to assume that above this frequency results are a good approximation. Below 2.3 kHz, results should be regarded as inaccurate unless proven otherwise.

The other assumption is that the boundaries are perfectly rigid, and any absorption is attributed to a real quantity which is not a function of angle of incidence. This results solely in a change of amplitude to the reflected wave. In practice, both magnitude and phase are affected. In order to model this phenomenon more accurately, each boundary wall has to be assigned an acoustic admittance (assuming local reactance), and each reflection has to be characterised by the angle it makes with the surface[13].

3. RESULTS AND DISCUSSION

The following results are presented in terms of the beamformer error (in dB), and plotted on a linear frequency scale[6]. The beamformer error is defined as $10\log\left(\frac{Y_{\text{opt}}}{|q_s^* q_s|}\right)$.

3.1. CSM Diagonal Replacement (DR)

Fig. 2 shows the effect of applying the CSM DR technique for data contaminated with maximum *(a)* 100,000% and *(b)* 10,000% noise when using a 112-channel array. The inherent improvement in signal-to-noise ratio of the 112-microphone array is evident as a 20 dB reduction in the error when compared to the single microphone case. In both cases, the diagonal removal technique reduces the error by another 10 dB (approx.), which would be equivalent to a further tenfold increase in channel count. With a 56-channel microphone array (not shown), the average errors are approx. 3 dB higher. There was no noticeable advantage of using either diagonal replacement with a column average or replacement by zeros (not shown in the plots). Of special concern is the large "uncertainty" in the beamformer levels when using the CSM optimisation techniques, which highlights the importance of averaging within sufficiently wide frequency bands when extracting absolute levels from beamforming results.

The sensitivity of the CSM DR technique to errors in $\vec{y}_p$ and $\vec{M}$ is presented in Fig. 3. Errors in $\vec{y}_p$ depend on the resolution of the grid points at the beamformer's scan plane. Errors in the Mach number are due to a local flow speed which varies from the free-stream velocity. The resulting beamformer error due to errors in $\vec{y}_p$ is a function of frequency, and the DR technique has very little effect on this error. Similar behaviour can be observed for errors in $\vec{x}_m$. Errors in $\vec{M}$ (plot *(b)*) give rise to much more significant beamformer errors. An error in Mach number corresponds to beamforming to a location other than the source position; in this case the 50% error corresponds roughly to a translational error of 0.12 m. The error

[6] A linear abscissa was chosen because *(a)* beamforming is most useful at high frequencies and *(b)* results at low frequencies can be inaccurate, as discussed in Section 2.4.

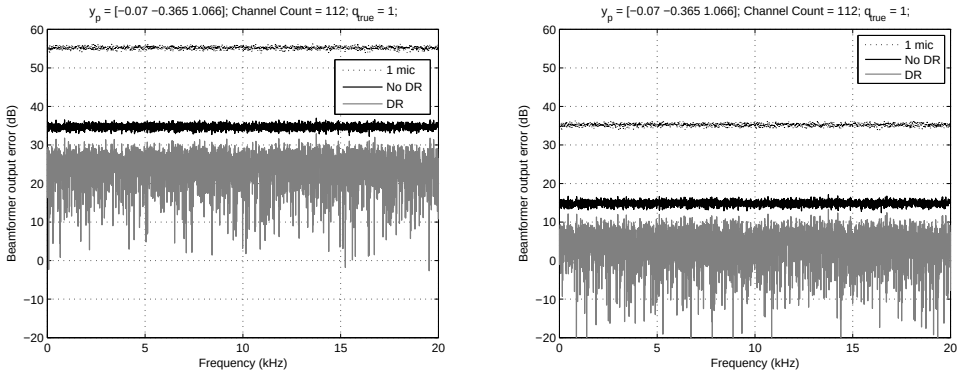

(a) 100,000% noise (b) 10,000% noise

Figure 2. Error in beamformer due to pressure data contaminated with the specified amount (maximum) of noise, with and without CSM DR. Free-field conditions. The output from a single microphone is included for comparative purposes.

curve is indirectly representing the beamformer's ability to suppress sources off the focus point, with higher performance at higher frequencies. Replacing the CSM diagonal gives larger error, however this can also be interpreted as lower sidelobes in the overall beamforming plot. Errors in Mach number can be easily avoided by extracting levels from the apparent source location on the beamformer plots, rather than the true source location.

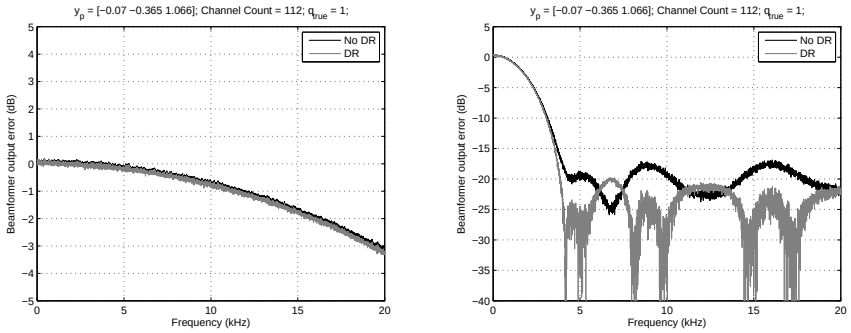

(a) Error of 0.01 m in $\vec{y}_p$ (b) Error of 50% in $\vec{M}$

Figure 3. Sensitivity of DR technique to errors in source location and Mach number. Free-field conditions. (a) no flow; (b) $\vec{U}$ = [80,0,0] m/s.

3.2. De-reverberation

To recreate a typical sound field in a hard-walled wind tunnel test section, an image source model as described in Section 2 was used to generate the simulated pressures. Beamforming was then carried out using either free-space Green's functions, or modified Green's functions as defined in equation 4. In order to give more realistic results, small errors where introduced in both $\vec{y}_p$ and $\vec{x}_m$. The resulting beamformer errors, with and without CSM DR, are shown in Fig. 4.

Standard beamforming overestimates the source strength by 10 to 20 dB; this can be attributed partly to the injected noise and partly to the reverberant field which increases the sound pressure at the microphones. Using de-reverberation, the error is reduced to an average of 2 dB.

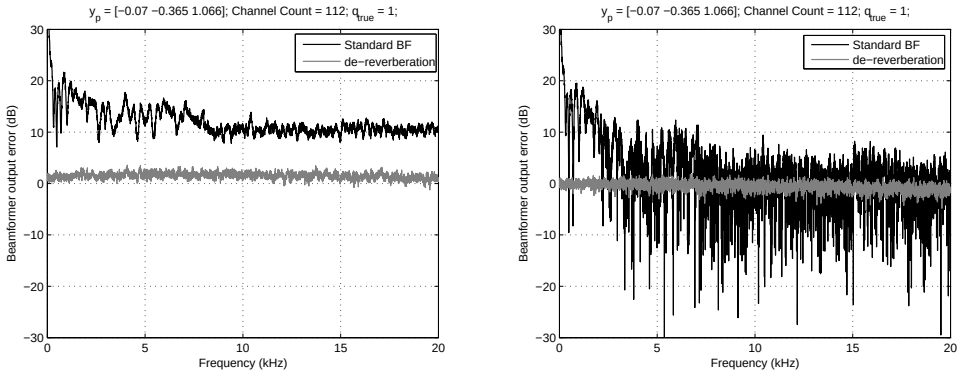

(a) Without diagonal replacement.

(b) With diagonal replacement.

Figure 4. Error in beamformer when beamforming in a reverberant space using free-space Green's functions (standard BF) and de-reverberation. 1000% noise, errors of 0.005 m in $\vec{y}_p$ and 0.001 m (max.) in $\vec{x}_m$. Reverberant sound field created using a first order ISM.

With CSM DR, the standard beamformer's error is reduced at high frequencies, at the expense of a large uncertainty in the measurements. CSM DR applied to de-reverberation reduces the error to ± 1 dB.

The image source model, on which de-reverberation is based, relies on the accurate location of the true source with respect to the wind tunnel boundaries in order to give accurate results. Therefore, it can be expected that de-reverberation will be particularly sensitive to errors in source position and wind tunnel cross-section. Fig. 5 confirms that de-reverberation is (a) quite robust to errors in $\vec{y}_p$ (similar performance to free-field conditions) and (b) more sensitive to errors in wind tunnel configuration at very high frequencies. Similar behaviour was observed with arrays having twice the aperture and different sensor distributions, and with a source at a different location (not shown).

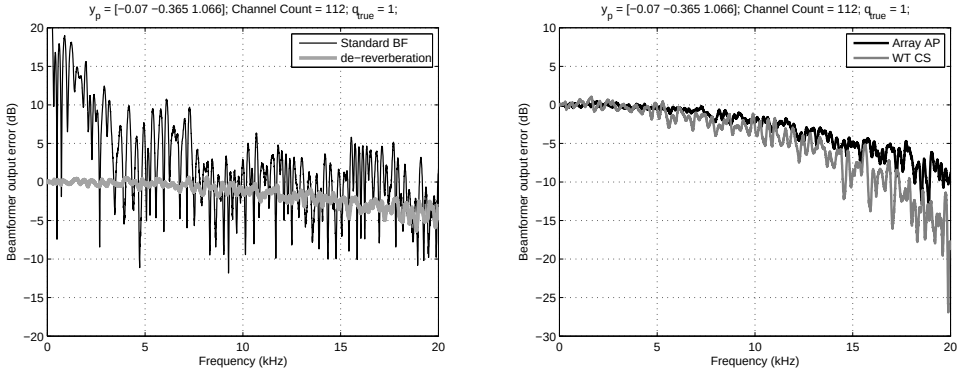

(a) Errors of 0.01 m in the x, y and z components of $\vec{y}_p$.

(b) Errors of 0.01 m in wind tunnel cross-section and absolute position of array.

Figure 5. Sensitivity of de-reverberation to position errors. 112-channel array, 100% noise contamination, ISM order 1, no flow. Plot (a) shows a comparison between standard beamforming and de-reverberation while (b) shows the sensitivity of de-reverberation to errors in absolute position of the array in the wind tunnel (Array AP) and wind tunnel cross-section (WT CS).

4. CONCLUSIONS

The accuracy of microphone array measurements in hard-walled wind tunnels is of particular concern, due partly to high levels of noise contamination at the array microphones, at the reverberant field. Altering the diagonal of the cross-spectral matrix has been shown to offer an additional reduction of up to 10 dB in the beamformer error to the standard reduction associated with the beamforming processing. However, for very high noise levels, the DR technique is not sufficient to nullify the error. In such circumstances, physically reducing the noise levels by, for example, recessing the array behind a tightly-stretched porous cloth [14] is recommended.

De-reverberation has been shown to be effective to improve the beamformer's accuracy by up to 10 dB, when measuring in a reverberant space. Accurate results can be expected at low to medium-high frequencies, even when small errors in source/receiver positions and wind tunnel geometry are present. At very high frequencies, this method becomes sensitive to position errors, especially the wind tunnel geometry.

ACKNOWLEDGEMENTS

This work is funded by the UK Engineering and Physical Sciences Research Council under grant GR/S68446/01. The authors wish to thank Phil Nelson, Keith Holland and Malcolm Smith of the Institute of Sound and Vibration Research, for many interesting discussions.

REFERENCES

[1] W. Humphreys Jr., T. F. Brooks, W. W. Hunter Jr., and K. R. Meadows. Design and use of microphone directional arrays for aeroacoustic measurements. *AIAA*, 98-0471, 1998.

[2] W. Dobrzynski, L. C. Chow, P. Guion, and D. Shiells. A European study on landing gear airframe noise sources. *AIAA*, 2000-1971, 2000.

[3] M.G.Smith, B. Fenech, L.C. Chow, N. Molin, W. Debrzynski, and C. Seror. Control of noise sources on aircraft landing gear bogies. *AIAA*, 2006-2626, 2006.

[4] P.T. Soderman et al. Airframe noise study of a CRJ-700 aircarft model in the NASA Ames 7- by 10- foot wind tunnel no. 1. *AIAA*, 2002-2406, 2002.

[5] G. Wicken and N. Lindener. The Audi aeroacoustic wind tunnel: Final design and first operational experience. *SAE*, 2000-01-0868, 2000.

[6] KR Holland and PA Nelson. Sound source characterisation: The focussed beamformer vs the inverse method. In *Tenth International Congress on Sound and Vibration*, July 2003.

[7] D. F. Long. Acoustic source location in wind tunnel tests via subspace BF. *AIAA*, 2003-0369, 2003.

[8] T. J. Mueller, editor. *Aeroacoustic Measurements*. Springer, 2002.

[9] B. Fenech and K. Takeda. Towards more accurate beamforming levels in closed-section wind tunnels via de-reverberation. *AIAA*, 2007-3431, 2007.

[10] A. D. Pierce. *Acoustics - An Introduction to Its Physical Principles and Applications*. ASA, 1994.

[11] P. Sijtsma. Experimental techniques for identification and characterisation of noise sources. NLR, 2004.

[12] B. Fenech and K. Takeda. SotonArray — Southampton University wind tunnel microphone array system guide. Technical Report AFM 07/03, SES, University of Southampton, 2007.

[13] P. M. Morse and K. U. Ingard. *Theoretical Acoustics*. Princeton University Press, 1986.

[14] S.M. Jaeger, W.C. Horne, and C.S. Allen. Effect of surface treatment on array microphone self-noise. *AIAA*, 2000-1937, 2000.